

How strongly can calcium ion influence the hydrogen-bond dynamics at complex aqueous interfaces?

Sanjib Senapati^{a)}

Department of Biotechnology, Indian Institute of Technology, Madras, Chennai 600036, India

(Received 12 February 2007; accepted 13 April 2007; published online 30 May 2007)

The author has performed three independent molecular dynamics computer simulations to examine the effects of counterion identity on hydrogen-bond dynamics in the enclosed water pool of anionic surfactant-based reverse micelles. The water–water hydrogen-bond lifetime in the reverse micelle (RM) with calcium ions is found to be longer than that in the RM with sodium or ammonium ions. The hydrogen bond between a polar head group and a water molecule, on the other hand, breaks but reforms most rapidly in the RM with calcium ions, indicating that there exists a strong competition between head group–counterion and head group–water interactions at such complex interfaces.

© 2007 American Institute of Physics. [DOI: 10.1063/1.2737053]

I. INTRODUCTION

The processes of breaking and making hydrogen bonds play a crucial role in the dynamical behavior of liquid water.^{1–4} The study of hydrogen-bond (H-bond) dynamics in aqueous solutions and at complex aqueous interfaces has therefore become a subject of intense current interest.^{5–11} Thus, Kropman and Bakker reported the direct measurement of the H-bond dynamics of water molecules solvating a Cl[−], Br[−], or I[−] anion by femtosecond midinfrared nonlinear spectroscopy.⁵ Chandra⁶ has performed a series of molecular dynamics (MD) simulations to study the effects of ion atmosphere on the H-bond dynamics in aqueous electrolyte solutions. Balasubramanian *et al.*⁷ have studied the dynamics of hydrogen bonds near a micellar surface by MD simulations. Hydrogen-bond kinetics in the solvation shell of a polypeptide⁸ and near the solvated biomolecules^{9,10} is also investigated computationally. A very recent work in this area involves the study of H-bond dynamics inside carbon nanotubes.¹¹ Most of these studies indicated a slower H-bond dynamics of water molecules in the first hydration shell than water molecules in the pure liquid.

Aqueous reverse micelles constitute another good example of complex interfaces, where nanometer-sized pools of water get stabilized in a hydrophobic solvent by a surfactant coat. The mobility and structure of this confined water were intensely studied both experimentally and with MD simulations in recent past.^{12–17} Experimental measurements based on quasielastic neutron scattering, electron spin resonance, nuclear magnetic resonance (NMR), IR vibrational echo peak shift, etc., have indicated that the translational and rotational mobilities of water molecules in RMs are much smaller than for bulk water.^{12–15} Computer simulations of aqueous RMs have also suggested that the interfacial waters become immobilized by a strong interaction with the ionic components at the interface.^{12,16,17} In a recent study on the effects of counterion identity on water mobility, Faeder *et al.*

have found that the interfacial mobility of water molecules in RMs is quite different for the counterion types and these differences are strongly correlated with ion–water coordination and the extent of disruption by the counterions of the water hydrogen-bond network.¹⁷ However, no study has yet been carried out to investigate the breaking and making dynamics of hydrogen bonds near a reverse micellar surface and, more importantly, the calcium ion induced changes of H-bond structure and dynamics at complex aqueous interfaces. Note that calcium ion has an unusual importance in biological phenomenon and a reverse micellar system serves as a prototype of more complex biological systems, in addition to being important in its own right.¹⁸ We shed some light on these issues by carrying out three MD simulations of ionic surfactant-based RMs.

II. BASIC MODELS AND SIMULATION DETAILS

The reverse micellar systems of our interest are composed of anionic perfluoropolyether carboxylate surfactant CF₃–(O–CF₂–CF(CF₃))₃–O–CF₂–COO[−] (PFPECOO[−]), water, and supercritical carbon dioxide as the hydrophobic solvent. The different counterions used in the calculations are NH₄⁺, Na⁺, and Ca⁺⁺. That perfluoropolyether-based microemulsions can produce thermodynamically stable aqueous domain in CO₂ phase is well proven by recent experimental¹⁹ and computational²⁰ studies. The water to surfactant mole ratio (W_o) was taken to be 8.4 and the simulations were carried out at 25 °C and 200 bar pressure. These values for the temperature, pressure, and W_o are the same as the values present in a recent NMR experiment of water transport in water-in-CO₂ microemulsions.¹⁹ All the three systems we simulated contained 554 water molecules, 66 fluorinated surfactant molecules, 6359 CO₂ molecules, and 66 counterions (33 in case of RM with Ca⁺⁺ ions). The number of surfactant and water molecules were again obtained based on the experimental parameters from Ref. 19. We started our simulations from an aggregated configuration, in which we distributed the surfactant molecules around the periphery of a sphere containing water molecules. The sur-

^{a)}Tel.: +91-44-2237-4122; Fax: +91-44-2257-4102; Electronic mail: sanjibs@iitm.ac.in

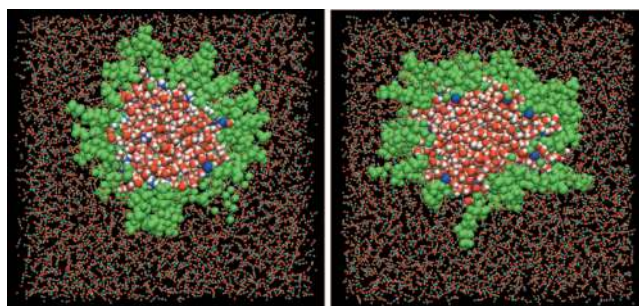


FIG. 1. (Color) Snapshots of the cross section of the micellar systems with NH_4^+ (left) and Ca^{++} (right) ions at 5 ns. Color scheme: red balls; water oxygens; white balls; either water or ammonium hydrogens; green balls; surfactants; blue balls; either calcium or nitrogen of the ammonium cations. The atoms of solvent molecules are represented by smaller circles with cyan and red color representing the carbon and oxygen atoms in CO_2 .

factants had their head groups pointed inward and their tails solvated in CO_2 pointed outward. The counterions were randomly added inside the sphere of water. To enable volume variation, the simulations were performed in the NPT ensemble using the Nose-Hoover thermostat and barostat. The production run was carried out for 5 ns after an equilibration phase of 500 ps in each system. A snapshot picture of the cross section of the NH_4^+ and Ca^{++} ion-based systems at 5 ns is presented in Fig. 1. We also have simulated a system containing pure bulk water at the same temperature and pressure as in simulations of micellar systems, so that the behavior of water in the confined system can be compared with that in the bulk phase.

The well-tested extended simple point charge model was chosen to describe the water molecules and an all atom approach is followed to model the anionic part PFPECOO^- of the surfactant.²¹ The optimized potential for liquid simulations set of intermolecular parameters has been used to model the counterions. The rigid rescaled elementary physical model²² proposed by Harris and Yung is used to describe CO_2 . Periodic boundary conditions were employed in all directions and the calculation of the long-range Coulombic forces was performed using the smooth particle mesh Ewald method. The real space part of the Ewald sum and Lennard-Jones interactions were cut off at 10 Å. All the simulations in this work were carried out using the DLPOLY (Ref. 23) molecular dynamics simulation package. Other details of the simulations can be found from our recent work on the water states in perfluoropolyether-based reverse micelles of varying counterion type²¹ (Paper I).

The results of Paper I can be summarized as the following: the reverse micelles remained stable over the 5 ns time period of the simulations. The radii of the aqueous core (R_c) obtained from NH_4^+ , Na^+ and Ca^{++} ion-contained RMs were 19.2 ± 0.5 , 18.6 ± 0.7 , and 18.9 ± 0.9 Å, respectively. The value of $R_c = 19.2$ Å is in a good agreement with the experimental value of 20 Å obtained for the aqueous droplet in $\text{PFPECOO}^- \text{NH}_4^+ / \text{water} / \text{carbon dioxide}$ system.¹⁹ The calculated values of micelle eccentricity and visual inspection implied that the reverse micelles in our simulations were essentially spherical. The orientational dynamics of water inside the reverse micelles was slower compared to the dynamics in bulk water irrespective of the type of the counterion present

in the solution. However, the water dynamics got slower as we progressed from NH_4^+ ion to Na^+ ion and finally to the Ca^{++} ion. These observations were consistent with the conclusions reached by Riter *et al.* in their experimental work performed on the sodium bis(2-ethylhexyl)sulfosuccinate reverse micelles.¹³

III. RESULTS AND DISCUSSIONS

Our analysis of H-bond dynamics was based on the construction of a hydrogen-bond population variable $h(t)$ which is unity when a particular tagged pair is hydrogen bonded at time t and zero otherwise. We follow the dynamics of hydrogen bonds among water molecules themselves and with the polar head groups at the reverse micellar surface. Note that the carboxylate head groups of the surfactant molecules contain oxygen atoms that are capable of forming hydrogen bonds with the first shell water hydrogens. We adopted a geometric definition of hydrogen bonding,^{1,6} according to which, a pair of water molecules is hydrogen bonded if the oxygen-oxygen distance is less than 3.5 Å and simultaneously the oxygen-oxygen-hydrogen angle is less than 30°. To describe a water-to-head-group hydrogen bond we have used the same geometric definition, i.e., a water and a head group are hydrogen bonded if a head group oxygen-water oxygen distance is not greater than 3.5 Å and simultaneously the head group oxygen-water oxygen-hydrogen angle is not greater than 30°. The structural relaxation of hydrogen bonds was then characterized by the hydrogen bond time correlation functions $C_{\text{HB}}(t)$ and $S_{\text{HB}}(t)$. The intermittent hydrogen bond correlation function $C_{\text{HB}}(t)$ can be defined as

$$C_{\text{HB}}(t) = \langle h(0)h(t) \rangle / \langle h \rangle, \quad (1)$$

where $h(t)$ is unity when a particular pair (either water-water or water-head group) is hydrogen bonded at time t , and zero otherwise. The angular brackets denote averaging over initial time values and over all pairs. The correlation function $C_{\text{HB}}(t)$ describes the probability that a pair of hydrogen-bonded molecules at time $t=0$ is also hydrogen bonded at time t , independent of possible breaking in the interim time. The correlation function $S_{\text{HB}}(t)$ defined as

$$S_{\text{HB}}(t) = \langle h(0)H(t) \rangle / \langle h \rangle, \quad (2)$$

where $H(t)$ is unity if the hydrogen bond of tagged pair remains continuously hydrogen bonded during the time duration t , and zero otherwise. The correlation function $S_{\text{HB}}(t)$ describes the probability that an initially hydrogen bonded pair remains bonded at all times up to t . Thus $S_{\text{HB}}(t)$ denotes a more accurate representation of the lifetime dynamics of the hydrogen bond, and the associated relaxation time τ_{HB} can be interpreted as the average lifetime of a hydrogen bond.⁶

To compare the water H-bond dynamics in the vicinity of the head group surface with the dynamics far from the surface, we have divided the water core into three regions. These regions were selected from the radial distribution function (rdf) between the carboxylate head group carbon and water oxygen. Region I contains interfacial water molecules that interact directly with the ionic components of the

TABLE I. Number of hydrogen bonds per water molecule. Error ranges are determined by calculating hydrogen-bond distributions for ten separate 100 ps segments.

Cation type	Region I	Region II	Region III
NH_4^+	1.723 ± 0.014	2.758 ± 0.032	3.501 ± 0.019
Na^+	1.869 ± 0.021	3.075 ± 0.042	3.514 ± 0.084
Ca^{++}	1.946 ± 0.042	3.249 ± 0.019	3.560 ± 0.016

surfactants, region II contains water molecules which lie between the first and second minima in the rdf, and the rest are region III water molecules. In Table I, we have shown the distribution of average number of H bonds per water molecule (n_{HB}) at various regions. The results show that the water-water H-bond pattern modifies significantly, particularly at the interface.²⁴ It also shows that the average number of H bonds is always larger for the RM with Ca^{++} counterion compared to other two RMs. This is somewhat surprising, since the ions having the highest charge densities (charge density order: $\text{Ca}^{++} > \text{Na}^+ > \text{NH}_4^+$) are expected to be the most disruptive of the water-water hydrogen bonding pattern. To explain this observation, we notice that the RM with calcium ions contains only half a number of counterions and holds a larger amount of water molecules in region I compared to other two systems. Region I water molecules in this RM, therefore, can be somewhat better hydrogen bonded to each other. The observed higher number of H bonds for regions II and III water molecules is due to the fact that, as we will see shortly, almost all Ca^{++} ions reside in region I and therefore are less effective in disrupting the water-water hydrogen bonding network in these regions. Now coming back to the dynamics, we find that the relaxation of $C_{\text{HB}}(t)$ for water-water in region I is slower in the RM with calcium ions. This has been displayed in Fig. 2. The inset of Fig. 2 shows the same function between two water molecules that both exist at several regions in the calcium ion-contained RM. Here we see that $C_{\text{HB}}(t)$ relaxes slower as we approach the surface. This implies that the electric field associated with the surface charges has a stronger influence on water

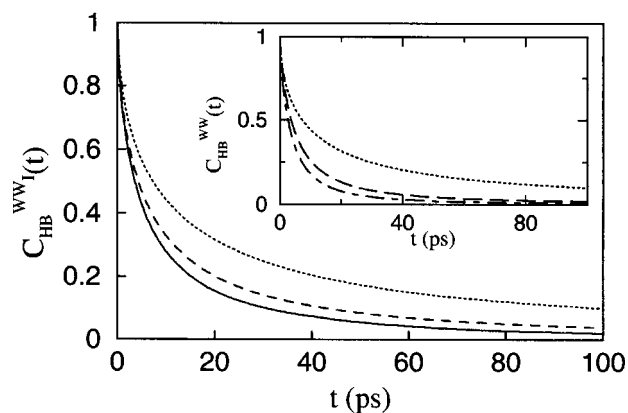


FIG. 2. The time correlation function, $C_{\text{HB}}(t)$, for the hydrogen bond between pairs of water molecules in region I. The solid, dashed, and dotted curves are for NH_4^+ , Na^+ , and Ca^{++} ion-contained RMs. The inset shows the same function between two water molecules that both exist at various regions in the RM with Ca^{++} ions; dotted curve: region I, long dashed curve: region II, and dot-dashed curve: regions III.

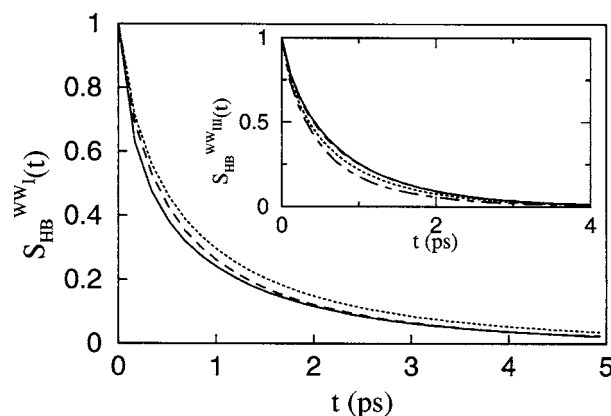


FIG. 3. The time dependence of $S_{\text{HB}}(t)$ for water-water in region I. The inset shows the same function for region III water molecules. The solid, dashed, and dotted curves are for the RM with NH_4^+ , Na^+ , and Ca^{++} ions. The dot-dashed curve in the inset shows $S_{\text{HB}}(t)$ for bulk water.

H-bond dynamics than the average number of hydrogen bonds per water molecule, n_{HB} has. In Fig. 3, we have displayed the time dependence of $S_{\text{HB}}(t)$ for water-water in all the three systems. A slower dynamics in Ca^{++} ion-based RM is again found, particularly for region I water molecules.²⁵ These correlation functions can be fitted to multiexponential function of the following form:

$$X_{\text{HB}}(t) = \sum_{i=1} c_i \exp(-t/\tau_i); \quad X_{\text{HB}} \equiv C_{\text{HB}} \text{ or } S_{\text{HB}}, \quad (3)$$

where $\sum_{i=1} c_i = 1$ and τ_i is the time constant for the decay of i th component. We could fit $C_{\text{HB}}(t)$ and $S_{\text{HB}}(t)$ to a sum of two/three exponents. The average time constants as obtained for region I water molecules from the multiexponential fit to $C_{\text{HB}}(t)$ are 11.65, 15.36, and 28.68 ps in the RM with NH_4^+ , Na^+ , and Ca^{++} ions. The water-water H-bond lifetimes in region I as calculated from the multiexponential fit to $S_{\text{HB}}(t)$ are found to be 0.81, 0.87, and 1.01 ps in the RM with NH_4^+ , Na^+ , and Ca^{++} ions. Thus the calcium ion-contained RM is found to have the slowest water-water hydrogen-bond relaxation and the longest water-water hydrogen-bond lifetime. Note that the average time constant in bulk water as obtained from the multiexponential fit to $C_{\text{HB}}^{\text{bulk}}(t)$ was 7.4 ps and the average lifetime of a water-water H bond in bulk water as obtained from the multiexponential fit to $S_{\text{HB}}^{\text{bulk}}(t)$ was 0.59 ps. A similar slowing down of water H-bond dynamics in the enclosed water pool of a nanometer-sized RM was recently reported by Tan *et al.*¹⁵ from their frequency resolved infrared vibrational echo experiments.

Now we switch our attention to the dynamics of water-head group (WHG) hydrogen bonds. In Fig. 4, we plot the relaxation of $C_{\text{HB}}^{\text{WHG}}(t)$ for all the three systems. This function again implies a stronger water-head group correlation in the RM with Ca^{++} ions. In all the systems, however, the decay is found to be nonexponential with a very slowly decaying tail. The longest time constant obtained from the multiexponential fit increases from 197 to 235 to 306 ps when we move from the RM with NH_4^+ to Na^+ to Ca^{++} ions (Table II). The strong water-head group interactions appear responsible for this slow hydrogen-bond dynamics, and is likely to be the origin of the universal slow relaxation at complex aqueous

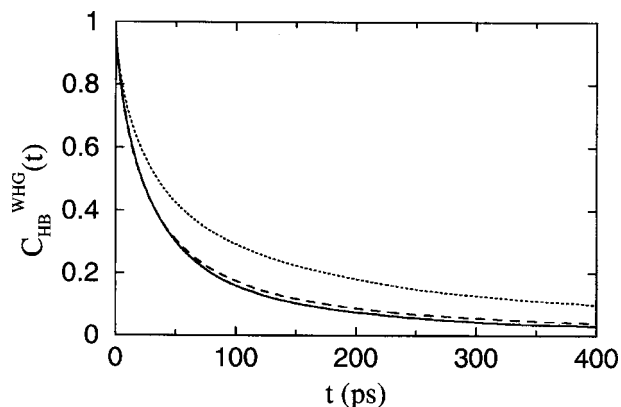


FIG. 4. The autocorrelation function, $C_{\text{HB}}(t)$, for the hydrogen bond between water and headgroups. The curve styles are the same as shown in Fig. 3.

interfaces that occurs on the similar 100–1000 ps time scale.¹³ The change in the values of the time constants implies that the water-counterion interactions are responsible for reducing a significant fraction of the water dynamics at such complex interfaces. The most important finding of this work, however, is presented in Fig. 5. Here we see that $S_{\text{HB}}^{\text{WHG}}(t)$ relaxes the fastest in the Ca^{++} ion-based RM. The water–head group H-bond lifetime in this RM is found to be shortened down by about 20% from the water–head group H-bond lifetime value of 3.92 ps in the NH_4^+ ion-contained RM.²⁶ This is in contrary to the results from Figs. 2–4, where the H-bond dynamics was the slowest in the RM with calcium ions. To explain this, we calculate the local densities of counterions as a function of distance from the effective surface formed by the carboxylate carbon atoms. The profiles are shown in Fig. 6. This figure clearly shows that all three types of cations have a tendency to form contact-ion pairs, and that calcium ions stay closest to the head group surface, followed by sodium and ammonium ions. The sharp and narrow peak observed for Ca^{++} counterions also indicates that in this case almost all of the ions remain ion paired with the head groups. The wider profiles for NH_4^+ and Na^+ ions, on the other hand, imply that in these cases quite a few ions dissociate from the surface and dissolve in the interior of the water pool. Indeed, it happens so as can be seen from Fig. 1.

The location of the ions and water molecules in the water pool is determined by a competition between the head group–ion, ion–water, and head group–water interactions. Ca^{++} ions with a high charge density can strongly interact with the polar head groups, and this may bring them closest

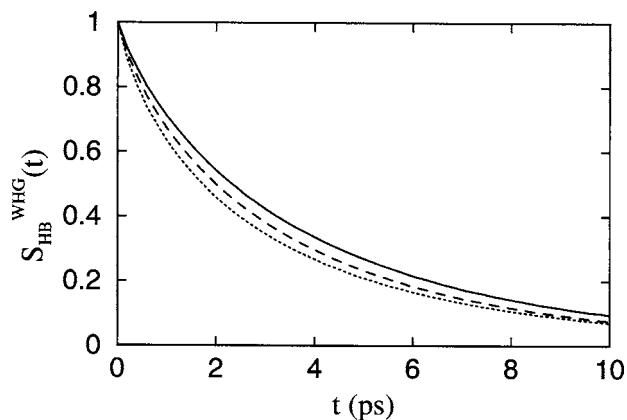


FIG. 5. $S_{\text{HB}}(t)$ function for the hydrogen bond between water and head groups. The curve styles are the same as shown in Fig. 3.

to the head groups. The closely residing Ca^{++} ions at the surface then can destabilize the water–head group hydrogen bonds relatively quickly to accomplish a shorter water–head group H-bond lifetime. Along similar lines, we found that the average number of water–head group hydrogen bonds per head group is reduced from 1.01 to 0.66 to 0.50 by going from the RM with NH_4^+ to Na^+ to Ca^{++} ions. Thus a faster decay of $S_{\text{HB}}(t)$ and a slower decay of $C_{\text{HB}}(t)$ indicate that the water–head group hydrogen bonds break but reform most rapidly in the calcium ion-contained RM. To support this we examine the trajectories of the individual water–head group pairs that were hydrogen bonded at time $t=0$. In Fig. 7, we plot the time evolution of the distances of four arbitrarily chosen pairs of this kind. The representative trajectories from NH_4^+ ion-contained RM [Figs. 7(a) and 7(b)] show that the water molecules remain hydrogen bonded to the respective head groups for some time before they go away from the surface. Once away, these water molecules show a less tendency to come back to the surface as they may find a stable environment under the influence of those NH_4^+ ions who were dissociated from the surface and dissolve in the interior of the pool. No such dissolved ion was present in Ca^{++} ion-based RM, instead all the Ca^{++} ions remained ion paired with the head groups (Fig. 6). Thus there exist two competing factors in the RM with Ca^{++} ions that influence the water molecules: (i) the proximity of the Ca^{++} ions to the head groups pushes the water molecules off the surface and (ii) the strong surface field generated by the head groups and Ca^{++} ions pulls the water molecules back to the surface. The trajectories from Ca^{++} ion-contained RM [Figs. 7(c) and 7(d)] reveal the occurrence of such events, where the water mol-

TABLE II. Fit parameters of the water–head group hydrogen-bond time correlation functions.

Function	Cation type	c_1	τ_1 (ps)	c_2	τ_2 (ps)	c_3	τ_3 (ps)
$C_{\text{HB}}^{\text{WHG}}(t)$	NH_4^+	0.28	5.65	0.54	36.23	0.18	197.60
	Na^+	0.32	6.58	0.49	38.91	0.19	235.29
	Ca^{++}	0.29	5.38	0.41	42.19	0.30	306.75
$S_{\text{HB}}^{\text{WHG}}(t)$	NH_4^+	0.06	0.34	0.27	1.80	0.67	5.10
	Na^+	0.08	0.30	0.29	1.63	0.63	4.74
	Ca^{++}	0.10	0.27	0.36	1.52	0.54	4.85

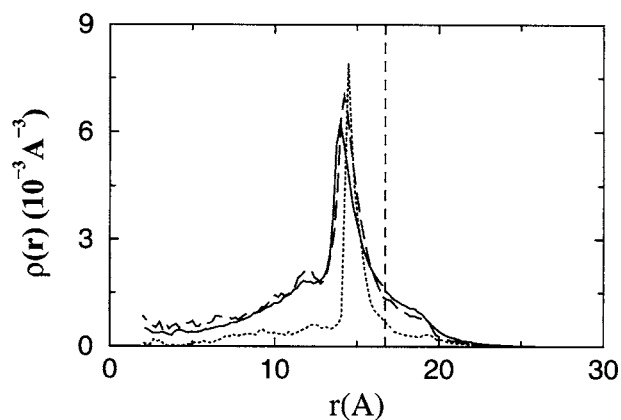


FIG. 6. Number density profiles for the NH_4^+ , Na^+ , and Ca^{++} ions in the corresponding RM with respect to the effective surface at 16.7 \AA (shown by a dashed vertical line). The effective surface is formed by the carboxylate carbon atoms. The curve styles are the same as shown in Fig. 3. (Adapted from Ref. ²¹ with permission.)

ecules clatter near the surface for some time, diffuse into the bulk region, and then revisits the surface to restore the hydrogen bonds with the head groups to which they were bonded at time zero. Note that there exist trajectories in the NH_4^+ ion-contained RM similar to the ones represented by Figs. 7(c) and 7(d) and there exist trajectories in the Ca^{++} ion-contained RM similar to the ones represented by Figs. 7(a) and 7(b). However, the analysis implied that the occurrence of such trajectories is much less probable than the trajectories corresponding to Fig. 7.

IV. SUMMARY AND CONCLUSIONS

In summary, we report on a computational study of the effect of counterion identity on hydrogen-bond dynamics in the water pool of a reverse micelle. The dynamics of water-water hydrogen bonds in the RM with calcium ions is seen to be slower compared to the dynamics in the RM with sodium or ammonium ions. The lifetime of the hydrogen bond between a water molecule and a surfactant head group is always found to be longer than that between two water mol-

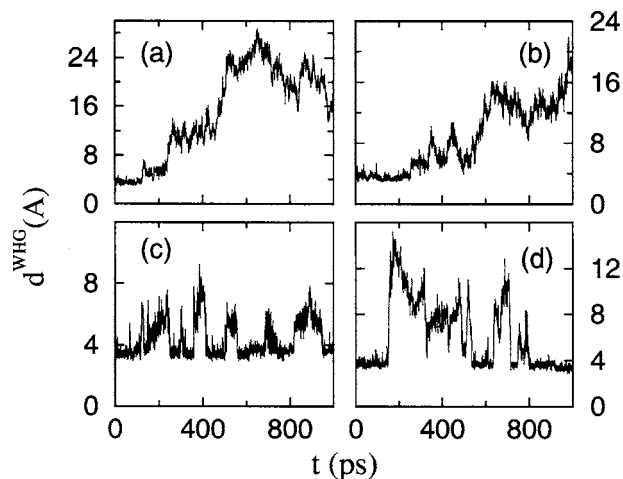


FIG. 7. Time evolution of the distances of arbitrarily chosen water-head group pairs that were hydrogen bonded at time zero; [(a) and (b)] from the RM with NH_4^+ ions [(c) and (d)] from the RM with Ca^{++} ions.

ecules. A strong interaction between head group-water and counterion-water appears responsible for this slow hydrogen-bond dynamics and is likely to be the origin of the universal slow relaxation of water dynamics at complex interfaces. We also found that there exist two competing factors in the RM with Ca^{++} ions that influence the water dynamics: (i) the proximity of the Ca^{++} ions to the head groups pushes the water molecules off the surface, leading to a rapid breaking of water-head group H bonds, and (ii) the strong surface field generated by the head groups and Ca^{++} ions pulls the water molecules back to the surface, leading to a rapid reformation of the broken hydrogen bonds. Thus, though the interfacial water molecules of Ca^{++} ion-contained RM have a shorter water-head group hydrogen-bond lifetime, they have the overall dynamics slower than the NH_4^+ or Na^+ ion-contained RM. We believe that our results are generic and should hold true for any complex aqueous interfaces including biomolecular surfaces containing polar regions.

ACKNOWLEDGMENTS

The author thanks Professor Max L. Berkowitz for helpful discussions and for allowing them to access the IBM SP machines at the North Carolina Supercomputing Center.

- ¹A. Luzar and D. Chandler, *Nature (London)* **379**, 55 (1996); *Phys. Rev. Lett.* **76**, 928 (1996).
- ²C. J. Fecko, J. D. Eaves, J. J. Loparo, A. Tokmakoff, and P. L. Geissler, *Science* **301**, 1698 (2003).
- ³J. B. Asbury, T. Steinell, C. Stromberg, K. J. Gaffney, I. R. Piletic, A. Goun, and M. D. Fayer, *Phys. Rev. Lett.* **91**, 237402 (2003).
- ⁴F. W. Starr, J. K. Nielsen, and H. E. Stanley, *Phys. Rev. Lett.* **82**, 2294 (1999).
- ⁵M. F. Kropman and H. J. Bakker, *Science* **291**, 2118 (2001); H. J. Bakker, M. F. Kropman, A. W. Omta, and S. Woutersen, *Phys. Scr.* **69**, C14 (2004).
- ⁶A. Chandra, *Phys. Rev. Lett.* **85**, 768 (2000).
- ⁷S. Balasubramanian, S. Pal, and B. Bagchi, *Phys. Rev. Lett.* **89**, 115505 (2002).
- ⁸H. Xu and B. J. Berne, *J. Phys. Chem. B* **105**, 11929 (2001).
- ⁹Y. Cheng and P. J. Rossky, *Nature (London)* **392**, 696 (1998).
- ¹⁰M. Tarek and D. J. Tobias, *Phys. Rev. Lett.* **88**, 138101 (2002).
- ¹¹I. Hanasaki and A. Nakatani, *J. Chem. Phys.* **124**, 1747141 (2006).
- ¹²M. R. Harpham, B. M. Ladanyi, N. E. Levinger, and K. W. Herwig, *J. Chem. Phys.* **121**, 7855 (2004).
- ¹³R. E. Riter, E. P. Undiks, and N. E. Levinger, *J. Am. Chem. Soc.* **120**, 6062 (1998); R. E. Riter, D. M. Willard, and N. E. Levinger, *J. Phys. Chem. B* **102**, 2705 (1998).
- ¹⁴H. Hauser, G. Haering, A. Pande, and P. L. Luisi, *J. Phys. Chem.* **93**, 7869 (1989).
- ¹⁵H. Tan, I. R. Piletic, R. E. Riter, N. E. Levinger, and M. D. Fayer, *Phys. Rev. Lett.* **94**, 057405 (2005).
- ¹⁶J. Faeder and B. M. Ladanyi, *J. Phys. Chem. B* **104**, 1033 (2000); **109**, 6732 (2005).
- ¹⁷J. Faeder, M. V. Albert, and B. M. Ladanyi, *Langmuir* **19**, 2514 (2003); M. R. Harpham, B. M. Ladanyi, and N. E. Levinger, *J. Phys. Chem. B* **109**, 16891 (2005).
- ¹⁸*Reverse Micelles: Biological and Technological Relevance of Amphiphilic Structures in Apolar Media*, edited by P. L. Luisi and B. E. Straub (Plenum, New York, 1984).
- ¹⁹K. P. Johnston, K. L. Harrison, M. J. Clarke, S. M. Howdle, M. P. Heitz, F. V. Bright, C. Carlier, and T. W. Randolph, *Science* **271**, 624 (1996); K. Nagashima, C. T. Lee, B. Xu, K. P. Johnston, J. M. DeSimone, and C. S. Johnson, *J. Phys. Chem. B* **107**, 1962 (2003).
- ²⁰S. Senapati and M. L. Berkowitz, *J. Phys. Chem. B* **107**, 12906 (2003).
- ²¹S. Senapati and M. L. Berkowitz, *J. Phys. Chem. A* **108**, 9768 (2004).

²²J. Harris and K. H. Yung, *J. Phys. Chem.* **99**, 12021 (1995).

²³W. Smith and T. R. Forester, DLPOLY, 2.12 version, CCLRC, Daresbury Laboratory, 1999.

²⁴The average number of hydrogen bonds per water molecule in bulk water is 3.60 at the specified temperature and pressure.

²⁵Inset of Fig. 3, however, shows that $S_{\text{HB}}^{\text{WM}}(t)$ decays faster for the RM with Ca^{++} ions. This is because, as we will see shortly, in this case almost

all of the Ca^{++} ions remain in region I and therefore they have little effect on H-bond dynamics in region III. In the cases of NH_4^+ and Na^+ ions we observe that a few counterions dissolve in the interior of the water pool, and thus they can slow down the water dynamics in region III.

²⁶The average lifetimes for water-head group hydrogen bonds in the RM with NH_4^+ , Na^+ , and Ca^{++} counterions are 3.92, 3.48, and 3.19 ps, respectively (see Table II).

The Journal of Chemical Physics is copyrighted by the American Institute of Physics (AIP). Redistribution of journal material is subject to the AIP online journal license and/or AIP copyright. For more information, see <http://ojps.aip.org/jcpo/jcpcr/jsp>